

1

Detecting post-stroke aphasia

2

using EEG-based neural envelope tracking

3

of natural speech

4

5 Pieter De Clercq¹, Jill Kries¹, Ramtin Mehraram¹, Jonas Vanthornhout¹, Tom Francart¹

6

and Maaike Vandermosten¹

7

¹: Experimental Oto-Rhino-Laryngology, Department of Neurosciences, Leuven Brain

8

Institute, KU Leuven, Belgium

9

Version:

10

March 2023

11

Corresponding author:

12

Pieter De Clercq (pieter.declercq@kuleuven.be)

Abstract

13

14 After a stroke, approximately one-third of patients suffer from aphasia, a language disorder that impairs
15 communication ability. The standard behavioral tests used to diagnose aphasia are time-consuming,
16 require subjective interpretation, and have low ecological validity. As a consequence, comorbid cognitive
17 problems present in individuals with aphasia (IWA) can bias test results, generating a discrepancy between
18 test outcomes and everyday-life language abilities. Neural tracking of the speech envelope is a promising
19 tool for investigating brain responses to natural speech. The envelope of speech is crucial for speech
20 understanding, encompassing cues for detecting and segmenting linguistic units, e.g., phrases, words and
21 phonemes. In this study, we aimed to test the potential of the neural envelope tracking technique for
22 detecting language impairments in IWA.

23 We recorded EEG from 27 IWA in the chronic phase after stroke and 22 healthy controls while they
24 listened to a 25-minute story. We quantified neural envelope tracking in a broadband frequency range as
25 well as in the delta, theta, alpha, beta, and gamma frequency bands using mutual information analysis.
26 Besides group differences in neural tracking measures, we also tested its suitability for detecting aphasia
27 at the individual level using a Support Vector Machine (SVM) classifier. We further investigated the
28 required recording length for the SVM to detect aphasia and to obtain reliable outcomes.

29 IWA displayed decreased neural envelope tracking compared to healthy controls in the broad, delta, theta,
30 and gamma band, which is in line with the assumed role of these bands in auditory and linguistic pro-
31 cessing of speech. Neural tracking in these frequency bands effectively captured aphasia at the individual
32 level, with an SVM accuracy of 84% and an area under the curve of 88%. Moreover, we demonstrated
33 that high-accuracy detection of aphasia can be achieved in a time-efficient (5 minutes) and highly reliable
34 manner (split-half reliability correlations between $R=0.62$ and $R=0.96$ across frequency bands).

35 Our study shows that neural envelope tracking of natural speech is an effective biomarker for language
36 impairments in post-stroke aphasia. We demonstrated its potential as a diagnostic tool with high reliabil-
37 ity, individual-level detection of aphasia, and time-efficient assessment. This work represents a significant
38 step towards more automatic, objective, and ecologically valid assessments of language impairments in
39 aphasia.

40 **Keywords:** Aphasia, natural speech processing, neural envelope tracking, diagnostics

41 1 Introduction

42 Aphasia is an acquired language disorder impairing communication ability and is principally caused by
43 a stroke in the language-dominant left hemisphere (Papathanasiou and Coppens, 2017). The current
44 practice is to diagnose aphasia by means of behavioral language tests. However, these tests suffer from
45 influences of co-morbid motor and cognitive problems (Rohde et al., 2018) and of a low ecological validity
46 (Devanga et al., 2021; Wallace and Kimelman, 2013). Novel analysis techniques for EEG-data, i.e.,
47 neural tracking of speech (e.g., see Lalor et al. (2009); Brodbeck et al. (2022); Crosse et al. (2021)), allow
48 measuring brain responses while participants listen to natural speech, providing an ecologically valid
49 way to measure speech processing. In this study, we test the potential of these novel EEG analyses for
50 detecting language impairments in aphasia with high accuracy and in a time-efficient way.

51 The current standard for diagnosing aphasia is based on performance on behavioral language tests,
52 such as the Western Aphasia Battery (Kertesz, 1982), the Token test (de Renzi and Ferrai, 1978) or
53 a picture-naming test (Van Ewijk et al., 2020). Yet, these tests have several disadvantages. First,
54 behavioral testing is time-consuming, requiring active cooperation of the patient and scoring by the
55 clinician. Second, behavioral assessment can lead to inaccurate initial diagnoses due to concomitant
56 motor, memory, attention and executive impairments (Rohde et al., 2018), reportedly affecting over
57 80% of individuals with aphasia (IWA) (El Hachioui et al., 2014). Finally, language tests consist of
58 rather artificial tasks in which sounds, phonemes, words or short sentences are presented in isolation.
59 This contrasts with natural speech processing where language components interact, and higher-level
60 context integration takes place (Hamilton and Huth, 2018; Kandylaki and Bornkessel-Schlesewsky, 2019).
61 Consequently, there is a discrepancy between clinical assessment and a patient’s natural speech abilities
62 in everyday life (Lesser and Algar, 1995; Kim et al., 2022; Stark et al., 2021; Wallace and Kimelman,
63 2013).

64 EEG-based event-related potential (ERP) studies have been conducted to address limitations of behav-
65 ioral testing. Studies have shown that IWA exhibit altered ERP components such as the P1, N1, P2, N2,
66 P300, and N400 in response to language stimuli (Aerts et al., 2015; Becker and Reinvang, 2007; Ilvonen
67 et al., 2001; Ofek et al., 2013; Pulvermüller et al., 2004; Robson et al., 2017). Together with the potential
68 for automatic assessment that requires less active participation from the patient, these alterations suggest
69 that ERPs may have diagnostic value in aphasia (Cocquyt et al., 2020). Nonetheless, ERP paradigms
70 involve artificial language stimuli presented repeatedly to the participant, which questions the ecological
71 validity of the obtained outcomes (Le et al., 2018). Furthermore, previous ERP studies in aphasia have
72 not reported on the reliability of ERPs, the minimal required recording length and the sensitivity to
73 capture language impairments at the individual level.

74 Recent studies have investigated the EEG response to natural, running speech, which could open new
75 perspectives to studying natural speech processing in IWA. When listening to speech, the brain tracks

76 the temporal envelope, which contains essential cues for speech understanding. The envelope consists
77 of the slow-varying temporal modulations in the speech signal and encompasses cues for detecting and
78 identifying lexical units (i.e., phonemes, syllables, words and phrases) and prosody (Pelle and Davis,
79 2012). In fact, previous research showed that listeners can understand speech based on the low-frequency
80 temporal envelope only (Shannon et al., 1995). Neural envelope tracking can be measured by applying
81 encoding and decoding models on the stimulus and the recorded EEG. The level of tracking is reflected
82 in the extent to which the models can either predict the neural signals or decode the envelope. In a linear
83 (Crosse et al., 2021) or a mutual information-based (De Clercq et al., 2023) model, the neural tracking
84 outcomes can be visualized over time and space (i.e., EEG channels), obtaining response properties similar
85 to traditional ERP components (Brodbeck et al., 2022). The neural tracking technique is rapidly evolving
86 and has led to crucial new insights as to how natural speech is processed in the brain. Neural envelope
87 tracking is strongly related to speech understanding (Ding and Simon, 2013; Etard and Reichenbach,
88 2019; Kaufeld et al., 2020), and can be used to objectively quantify speech intelligibility (Vanthornhout
89 et al., 2018; Gillis et al., 2022).

90 Prior research assigned the low-frequency temporal envelope primarily to speech understanding. The
91 low-frequency envelope, i.e., delta (0.5–4 Hz) and theta (4–8 Hz) band, encompass cues for detecting and
92 segmenting lexical units. The theta band tracks syllables and lower-level acoustic processing of speech
93 (Etard and Reichenbach, 2019), while the delta band signal is associated with processing speech prosody
94 and segmenting higher-level linguistic structures such as words and phrases (Ding et al., 2016; Giraud
95 and Poeppel, 2012; Kaufeld et al., 2020). In addition to the delta and theta band, reflecting synthesis of
96 higher-level auditory and linguistic structures, the alpha and beta bands are involved in attention and
97 auditory-motor coupling (Wöstmann et al., 2017; Fujioka et al., 2015), while the gamma band is involved
98 in encoding phonetic features (Giraud and Poeppel, 2012; Gross et al., 2013; Hyafil et al., 2015). In
99 conclusion, specific frequency bands are believed to reflect different stages of speech processing.

100 Neural envelope tracking of natural speech has been investigated in several clinical populations with
101 language impairments. For individuals with primary progressive aphasia, a language disorder caused by
102 a neurodegenerative disease, Dial et al. (2021) reported increased neural tracking in the theta band but
103 no group differences in the delta band. The researchers argued that enhanced theta band tracking in
104 individuals with primary progressive aphasia might reflect a compensation mechanism through increased
105 reliance on acoustic cues. For individuals with dyslexia, a disorder characterized by phonological pro-
106 cessing difficulties, decreased tracking in delta, theta and beta/gamma (phoneme- and phonetic-level)
107 band have been reported (Di Liberto and Lalor, 2017; Lizarazu et al., 2021; Mandke et al., 2022). In
108 conclusion, these studies have shown the potential for neural tracking to capture language impairments
109 in clinical cohorts.

110 The present study investigated whether we can differentiate IWA in the chronic phase after stroke

111 (i.e., ≥ 6 months post-stroke) from neurologically healthy, age-matched controls using EEG-based neural
112 envelope tracking. Specifically, we used mutual information analyses to quantify neural envelope tracking,
113 which captures linear and nonlinear effects and outperforms linear models (De Clercq et al., 2023).
114 We described both groups' responses to the speech envelope temporally and spatially at broadband
115 frequency range. We further investigated neural tracking in specific frequency bands ranging from delta
116 to gamma band, as different frequency bands are involved in different (sub-)lexical processes (Etard and
117 Reichenbach, 2019; Ding et al., 2016; Giraud and Poeppel, 2012; Keitel et al., 2018; Peelle and Davis,
118 2012).

119 Secondly, we assessed the suitability of the neural tracking technique as a biomarker to capture language
120 processing difficulties. To this end, we used a Support Vector Machine (SVM) to classify participants
121 as healthy or aphasic using MI measures in different frequency bands as input to the model. Finally,
122 we investigated how much data the neural tracking technique requires for good classification and reliable
123 outcomes.

124 2 Materials and methods

125 2.1 Participants

126 Our sample comprised 27 IWA (seven female participants, 73 ± 11 y/o) in the chronic phase (≥ 6 months)
127 after stroke and 22 neurologically healthy controls (seven female participants, 72 ± 7 y/o). There was no
128 significant age difference between groups (unpaired Wilcoxon rank sum test: $W=343.5$, $p=0.36$). IWA
129 were recruited at the stroke unit of the University Hospital Leuven and via speech-language pathologists.
130 Healthy controls were recruited, making sure they matched the age of IWA at the group level. The
131 inclusion criteria for IWA were: (1) a left-hemispheric or bilateral stroke, (2) a diagnosis of aphasia in
132 the acute stage after stroke using behavioral language tests and (3) no formal diagnosis of a psychiatric
133 or neurodegenerative disorder. For more information regarding demographics, recruitment strategy and
134 diagnosis in the acute stage after stroke, we refer to Kries et al. (2022). The study was approved
135 by the ethical committee UZ/KU Leuven (S60007), and all participants gave written consent before
136 participation. Research was conducted in accordance with the principles embodied in the Declaration of
137 Helsinki and in accordance with local statutory requirements.

138 Participants completed standardized clinical tests for aphasia at the time of participation as described in
139 detail in Kries et al. (2022). IWA scored significantly lower on the 'Nederlandse Benoemtest', i.e., Dutch
140 Naming Test (Van Ewijk et al., 2020), and the ScreeLing test (El Hachoui et al., 2017; Visch-Brink
141 et al., 2010) compared to healthy controls ($W=57.5$, $p<0.001$; $W=101$, $p<0.001$, respectively). Although
142 seven IWA did not score below the cut-off threshold for aphasia on either of these tasks, they were still
143 attending speech-language therapy sessions at the time of participation and had extended documentation

144 of language deficits in the acute stage after stroke (Kries et al., 2022).

145 **2.2 EEG experiment**

146 The EEG measurements took place in a soundproof, electromagnetically shielded booth using a 64-
147 channel BioSemi ActiveTwo system (Amsterdam, the Netherlands) at a sampling frequency of 8,192 Hz.
148 Participants were instructed to listen to a 25-minute-long story, *De Wilde Zwanen*, written by Christian
149 Andersen and narrated by a female Flemish-native speaker, presented in silence while their EEG was
150 recorded. The story was cut into five parts with an average duration of 4.84 minutes. After each story part,
151 participants answered content questions about the preceding part, introduced to make the participant
152 follow the content attentively. Participants had a short break after each story part and answered content
153 questions about the preceding part. The protocol introduced these questions to make participants follow
154 the story attentively. The story was presented bilaterally through ER-3A insert earphones (Etymotic
155 Research Inc, IL, USA) using the software platform APEX (Francart et al., 2008).

156 We determined a subject-dependent intensity level at which the story was presented based on the
157 thresholds of the pitch tone audiometry (PTA). We defined hearing thresholds for octave frequencies
158 between .25 and 4 kHz. For normal hearing participants, the story was presented at 60 dBA. For hearing
159 impaired participants, defined as participants that have a hearing threshold >25 dB hearing loss on
160 frequencies below 4 kHz, the volume was augmented with half of the pure tone average of the individual
161 thresholds at .25, .5 and 1 kHz for both ears individually. This procedure was adapted from Jansen
162 et al. (2012). To check whether age-related hearing loss differed between both groups, we calculated the
163 Fletcher index, i.e., average of PTA thresholds at .5, 1 and 2 kHz. Hearing levels did not differ between
164 groups (Fletcher index averaged across the right and left ear: $W=326.5$, $p=0.56$).

165 **2.3 Signal processing**

166 **Envelope extraction**

167 We used a gammatone filter bank (Søndergaard et al., 2012) to extract the envelope. We used 28 channels
168 spaced by one equivalent rectangular bandwidth and center frequencies from 50 Hz until 5000 Hz. The
169 envelopes were extracted from each sub-band by taking the absolute value of each sample and raising it
170 to the power of 0.6. The resulting 28 sub-band envelopes were averaged to obtain a single envelope. Next,
171 the envelope was downsampled to 512 Hz to decrease processing time. The envelope was then filtered
172 in frequency ranges of interest. These include delta (0.5-4 Hz), theta (4-8 Hz), alpha (8-12 Hz), beta
173 (12-30 Hz), low-gamma (30-49 Hz) and a broad (0.5-49 Hz, including all individual frequency ranges)
174 band. We used high- and lowpass filters, with a transition band of 10% below the highpass and 10%
175 above the lowpass frequency. A Least Squares filter of order 2000 was used, and we compensated for the
176 group delay. After filtering, the envelope was normalized and further downsampled to 128 Hz.

177 EEG data processing

178 EEG data were pre-processed using the Automagic toolbox (Pedroni et al., 2019) and custom Matlab
179 scripts (The MathWorks Inc., Natick, MA, USA, 2021). The EEG signals were first downsampled to
180 512 Hz to decrease processing time. Artifacts were removed using the artifact subspace reconstruction
181 method (Mullen et al., 2015). Next, an independent component analysis was applied to the data, and
182 components classified as "brain" or "other" (i.e., mixed components), using the EEGLAB plugin ICLabel
183 (Pion-Tonachini et al., 2019), with a probability higher than 50% were preserved (average number of
184 removed components: 26 ± 7). The neural signals were projected back to the channel space, where the
185 signals were average referenced. Subsequently, we filtered the EEG data in the same frequency bands
186 using the same Least Squares filter as in the envelope extraction method. Next, normalization and further
187 downsampling to 128 Hz were applied.

188 2.4 Neural envelope tracking

189 We investigated neural envelope tracking using the Gaussian copula MI analysis (Ince et al., 2017). In
190 the Gaussian copula approach, all variables (the envelope and EEG channels) are first ranked on a scale
191 from 0 to 1, obtaining the cumulative density function (CDF). By computing the inverse standard normal
192 CDF, the data distributions of all variables are transformed to perfect standard Gaussians. Subsequently,
193 the parametric Gaussian MI estimate can be applied to the data provided by:

$$I(X; Y) = \frac{1}{2 \ln 2} \left[\frac{|\sum_X| |\sum_Y|}{|\sum_{XY}|} \right] \quad (1)$$

194 where $I(X; Y)$ equals the MI between X and Y (here, the EEG and the envelope), expressed in bits. $|\sum_X|$
195 and $|\sum_Y|$ are the determinants of the covariance matrices of X and Y , and $|\sum_{XY}|$ is the determinant of
196 the covariance matrix for the joint variable. To obtain temporal information on MI, we shifted the EEG
197 as a function of the envelope over time (using an integration window -200 to 500 ms) and applied Eq. (1)
198 at each sample. The result forms the temporal mutual information function (TMIF) and reflects how the
199 brain processes speech over time (De Clercq et al., 2023; Zan et al., 2020). For an in-depth explanation
200 of the Gaussian copula MI method, we refer to Ince et al. (2017). For a more practical explanation of
201 the TMIF in the context of neural envelope tracking, see De Clercq et al. (2023).

202 We calculated the single-channel TMIF and the multivariate TMIF, analog to a (linear) encoding and
203 decoding model, respectively. The single-channel TMIF calculates the TMIF for each channel individ-
204 ually, providing both temporal (i.e., peak latency and peak magnitude) and spatial (i.e., topography)
205 information on speech processing. Alternatively, the multivariate TMIF determines the multivariate re-
206 lationship between multiple EEG channels combined and the speech envelope. This latter method is
207 statistically more powerful as it takes interactions between EEG channels into account. However, it

208 is restricted to temporal interpretations only. For the multivariate TMIF, we used a channel selection
209 including fronto-central and parieto-occipital channels that contribute to speech processing (Lesenfants
210 et al., 2019). Our channel selection is visualized in Supplementary Fig. 1.

211 **Permutation testing**

212 Neural tracking (MI in bits, in this case) is a relative metric and should be compared to a null-distribution
213 to quantify the meaningfulness of the derived values (De Clercq et al., 2023). We created stationary noise
214 that matched the spectrum of the envelope per frequency band individually. Next, we calculated the
215 MI between the noise envelope and the EEG per participant and repeated this process 1000 times. The
216 significance level was then determined as the 95th percentile of permutations per participant (resulting
217 in a single significance level per participant).

218 No significant differences were found in the significance level between IWA and controls for any fre-
219 quency band, as determined by Wilcoxon rank sum tests. Supplementary Fig. 2 displays the significance
220 levels of the multivariate TMIF for all frequency bands categorized by group. As no significant differ-
221 ences in the significance level were found between groups, we used a single significance level (i.e., the
222 95th percentile of permutations across all participants) to interpret the multivariate TMIFs in the Results
223 section.

224 **2.5 Statistics**

225 **Group comparisons**

226 We compared neural envelope tracking for IWA with the control group for broadband as well as for
227 delta, theta, alpha, beta and gamma frequency ranges. For the single-channel TMIF, we performed non-
228 parametric spatio-temporal cluster-based permutation tests (Maris and Oostenveld, 2007), indicating
229 clusters in the TMIF over time and space with the largest group difference at threshold $p < 0.05$. For the
230 multivariate TMIF, we performed non-parametric temporal cluster-based permutation tests (Maris and
231 Oostenveld, 2007), indicating clusters of samples with the largest group difference at threshold $p < 0.05$.

232 **Support Vector Machine Classification**

233 We investigated whether EEG-based envelope tracking outcomes can be used for detecting aphasia. To
234 this end, we used a Support Vector Machine (SVM) to classify held-out participants as control or aphasic
235 using the Scikit-Learn (v. 0.24.2) library in Python (Pedregosa et al., 2011). The multivariate TMIFs
236 for all five individual frequency bands (delta to gamma) were used as input to the model. Additionally,
237 we added age of the participant, as it influences neural envelope tracking (Decruy et al., 2019). We
238 chose a radial basis function kernel SVM and performed a nested cross-validation approach. In the inner

239 cross-validation, the C-hyperparameter and pruning (i.e., length of the TMIFs) were optimized (accuracy-
240 based) and tested in a validation set using 5-fold cross-validation. The trained model was then tested on
241 the test set, for which we used a leave-one-subject-out cross-validation approach.

242 The performance of the SVM classifier was evaluated by computing the receiver operating characteristic
243 (ROC) curve and calculating the area under the curve (AUC). We further reported the overall accuracy,
244 the F1-score, the sensitivity and the specificity of the classifier.

245 **Feature contribution.** To obtain a proxy for the relevant contribution of each frequency band, we
246 left out a single band and re-fitted the SVM. We repeated this process for all five frequency bands and
247 reported the corresponding performance drop (AUC, accuracy, F1-score).

248 **Recording time**

249 **Classification.** From a practical perspective, we were interested in how much data the neural envelope
250 tracking technique requires to detect aphasia accurately and obtain stable, reliable results. We iteratively
251 cropped the EEG recording and the envelope in steps of 2 minutes (using the first 1 minute, first 3
252 minutes, 5, 7... up to the entire 25 minutes of recording time) and calculated the TMIF per frequency
253 band per time duration. Next, we investigated the amount of minutes required for the SVM to reach its
254 classification potential. As described above, we trained and tested our SVM per time duration in the
255 same fashion as the entire duration. Performance (AUC, accuracy, F1-score) was plotted as a function of
256 recording time. We determined the knee point, i.e., the point at which the performance benefit starts to
257 saturate, using the "kneed" python package (Satopaa et al., 2011). The knee point of this curve reflects
258 the point at which the increase in model performance may no longer be worth the corresponding effort.

259 **Within-subjects stability.** Second, we investigated the data required to obtain stable, reliable
260 results. We determined the within- and between-subjects stability per time duration. For the within-
261 subjects stability, we individually correlated (Pearson) the TMIF per time duration (i.e., first minute,
262 first 3, 5, ...) with the TMIF of the entire recording per subject. This resulted in a single correlation
263 coefficient for each participant, frequency band and time duration. Next, all correlations were plotted as
264 a function of recording time, and we determined the knee point of the curve on the average across all
265 frequency bands. As such, we gained insight into the amount of data required for a participant's TMIF
266 to become stable (i.e., when there is not much change in an individual's TMIF).

267 **Between-subjects stability.** For the between-subjects stability, we calculated each participant's
268 mean MI of the TMIF (integration window 0-400 ms) per time duration (1, 3, 5,... minutes) and the
269 entire recording. This resulted in a single datapoint per participant, frequency band and time duration
270 (i.e., mean MI for a certain duration length x mean MI entire duration). Subsequently, we calculated the
271 correlation coefficient (Pearson's R) between the mean MI for certain time duration and frequency band
272 with the entire recording over participants on the group level, resulting in a single correlation coefficient

273 per time duration and frequency band. We plotted the correlations as a function of recording time and
274 determined the knee point of the curve on the average across all frequency bands. With this analysis, we
275 investigated the amount of data required for a participant's relative (i.e., compared to other participants)
276 strength of tracking to become stable (i.e., from which point on a participant's relative neural tracking
277 compared to other participants is no longer expected to change).

278 **Split-half reliability**

279 Finally, we report a traditional split-half reliability metric with non-overlapping parts of the recording.
280 We split the EEG recording into two equal parts, i.e., the first 12.5 minutes and the second 12.5 minutes,
281 and computed the TMIFs for each half and each frequency band individually. Next, we computed the
282 mean MI value of the TMIF (0-400 ms) for the first and the second half of the recording per participant
283 individually. Subsequently, we calculated the correlation coefficient (Pearson's R) between the first and
284 second half of the recording over participants on the group level (Pearson's R) for IWA and controls
285 separately.

286 **Data availability statement**

287 We shared our neural tracking outcomes (i.e., the TMIFs) on the Open Science Framework: <https://osf.io/nkmfa/>. Note that our ethical approval does not permit public archiving of raw neuroimaging
288 data, but raw EEG data can be made available upon request and if the GDPR-related conditions are
289 met.
290 met.

291 **3 Results**

292 **3.1 Distinguishing individuals with aphasia from healthy controls**

293 We investigated whether neural envelope tracking is altered in IWA compared to healthy controls. First,
294 we studied the effect in the broadband frequency range (0.5-49 Hz). For the single-channel MI analysis,
295 providing both temporal and spatial information, we found decreased neural envelope tracking for IWA
296 compared to healthy controls (Fig. 1A). A spatio-temporal cluster-based permutation test identified a
297 cluster comprising a large group of fronto-central, parietal and posterior channels ($N = 43$ channels) from
298 0.11 s to 0.3 s ($p=0.004$), centered around the second peak. The multivariate MI analysis, which combines
299 information from multiple channels, confirmed these results: a temporal cluster-based permutation test
300 identified a cluster between 0.11 s to 0.26 s in which IWA displayed a decreased response ($p = 0.005$)
301 (Fig. 1B).

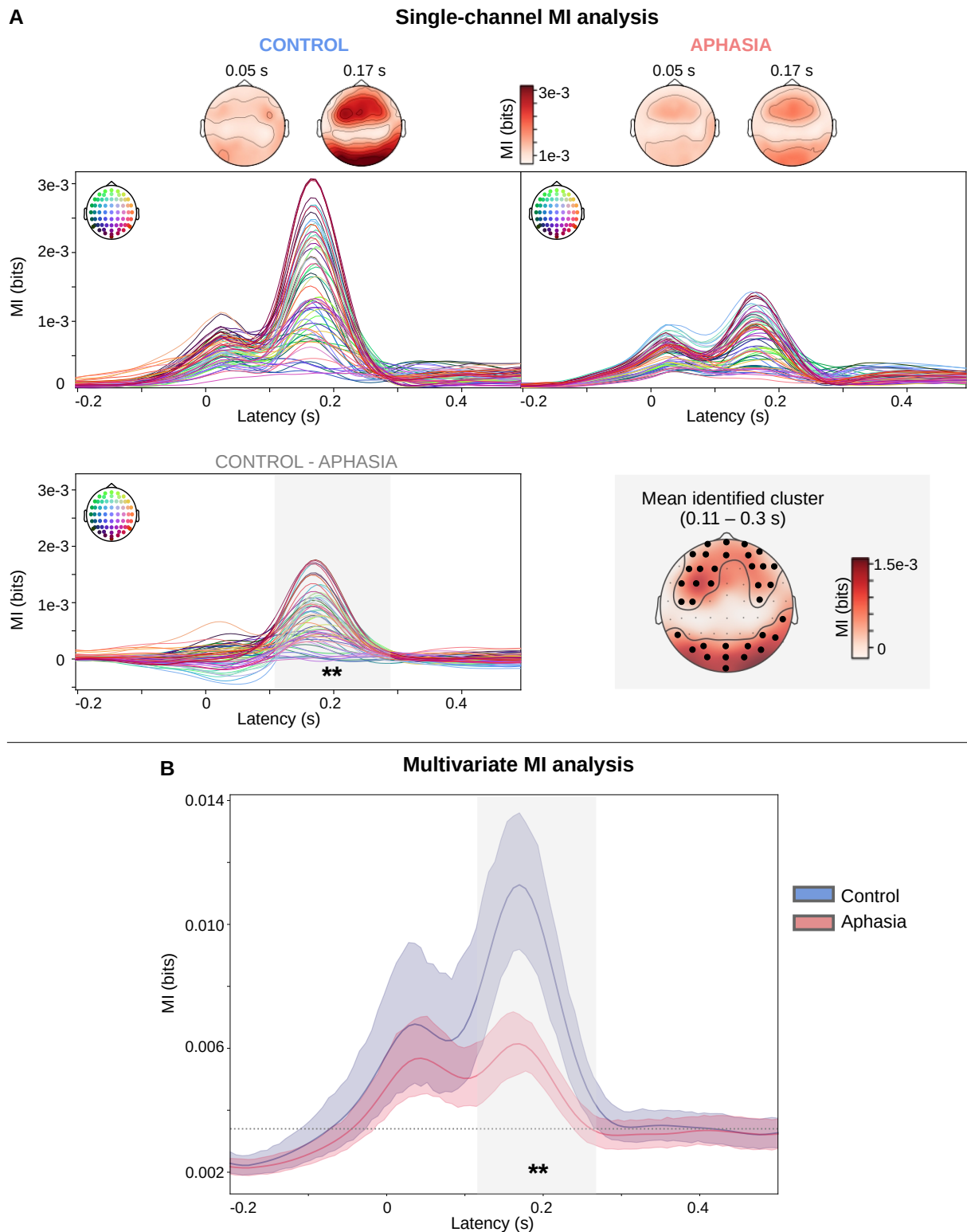


Figure 1. Broadband analysis. A. The average single-channel TMIF for the control and the aphasia group separately, with topoplots at the first and second peak (0.05 and 0.17 s). The spatio-temporal cluster-based permutation test investigated the difference between the control and aphasia group (control - aphasia) and identified a cluster (below threshold $p < 0.05$) with the largest group difference, centered around the second peak. Brain latencies belonging to the cluster are marked in a shaded gray area, the channels belonging to the cluster are indicated with a black dot on the topoplot. **B.** The group average TMIF, for both groups separately. The shaded, colored areas indicate the 95% confidence interval. The shaded gray area indicates the cluster with largest group difference (threshold $p < 0.05$), identified using a temporal cluster-based permutation test. ** = $p < 0.01$

302 We further investigated the neural response in narrow frequency bands. We focused on the multivariate
303 TMIF as it is a statistically more robust method compared to the single-channel TMIF, and we used
304 those features as input to our SVM classifier in the subsequent section. The single-channel TMIFs for all
305 frequency bands are provided in the Supplementary materials. We generally observed decreased neural
306 envelope tracking for IWA compared to healthy controls (Fig. 2). Temporal cluster-based permutation
307 tests identified clusters below threshold $p < 0.05$ for delta (0.1 to 0.30s, $p = 0.003$), theta (0.04 to 0.27s,
308 $p = 0.005$) and gamma (0.01 to 0.1s, $p = 0.004$) band. No clusters exceeding the $p < 0.05$ threshold were
309 detected for the alpha and beta bands. These results are confirmed in the single-channel MI analysis,
310 where spatio-temporal cluster-based permutation tests identified clusters for delta, theta and gamma
311 band for a large group of fronto-central, parietal and posterior channels (visualizations and statistics
312 provided in the Supplementary materials).

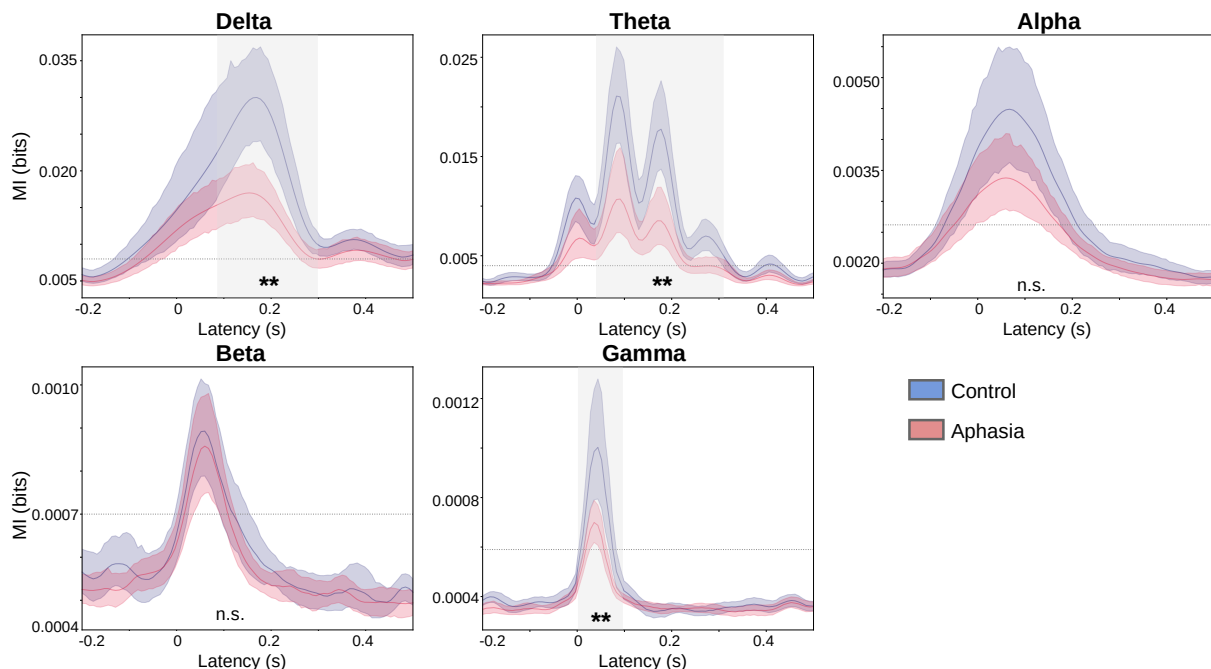


Figure 2. Frequency-specific analysis. Group average TMIF's visualized per frequency band, with colored shaded areas indicating the 95% confidence interval. Shaded, gray areas indicate clusters with largest group difference (below threshold $p < 0.05$) identified using temporal cluster-based permutation tests. ** = $p < 0.01$

313 3.2 Support Vector Machine classification

314 Next, we investigated whether we could detect aphasia based on neural envelope tracking measures in
315 the individual frequency bands. To this end, we used an SVM to classify participants as belonging to
316 the aphasia or the healthy control group via leave-one-out cross-validation. We used the TMIFs in our
317 five frequency bands of interest and age as input features to the model. The SVM successfully classified
318 participants belonging to either group with an accuracy of 83.67%, an F1-score of 83.58% and an AUC of
319 88.05%. The SVM had a sensitivity of 88.89% and a specificity of 77.27% for aphasia. Fig. 3A displays

320 the ROC curve.

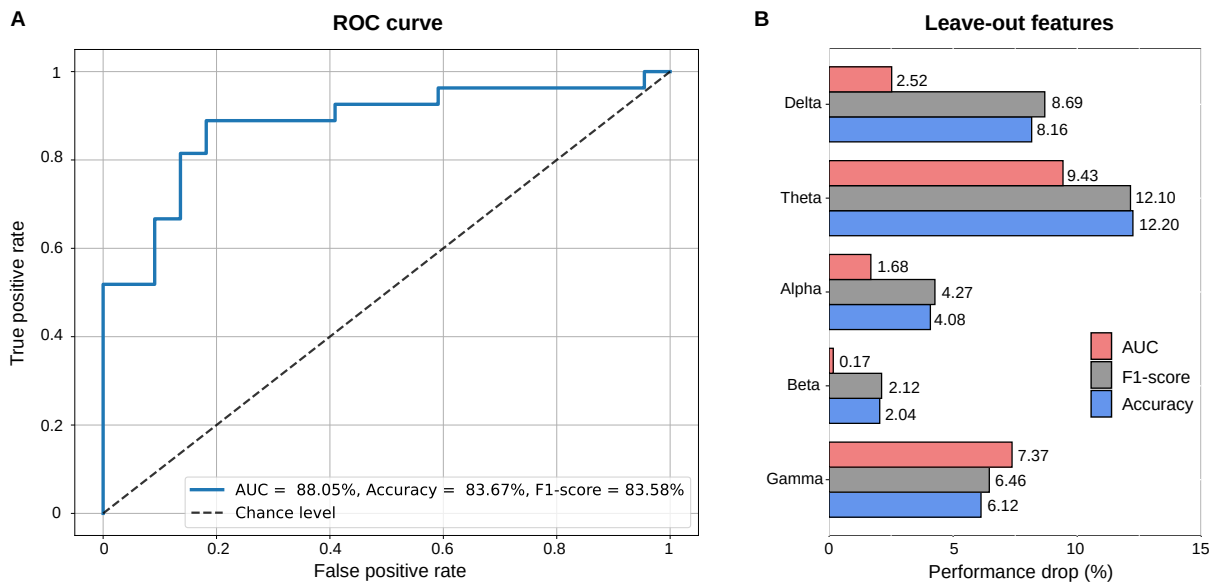


Figure 3. Result of the SVM classifier. A. Receiver operating characteristic curve (ROC). **B.** Relative feature importances. Drop in performance is visualized after leaving out the corresponding feature (i.e., frequency band).

321 To obtain a measure of relative frequency band contribution, we iteratively left out a frequency band
322 and trained the SVM with the remaining features. For each left-out frequency band, we calculated the
323 performance drop. As assessed with accuracy and F1-score metrics, theta, followed by delta, gamma,
324 alpha and beta caused the largest drop in performance (see Fig. 3B). When estimated with AUC, the
325 accuracy was still the highest for theta, followed by gamma, delta, alpha and beta. This confirmed our
326 group comparison analyses: delta, theta and gamma band are the most relevant, discriminating features.

327 3.3 Recording length

328 We further investigated how much data the neural envelope tracking technique requires for robust and
329 stable results (Fig. 4). With only one minute of recording time, the SVM obtained classification accuracy
330 close to chance-level (55%). Yet, from 5 minutes on, the SVM reached an accuracy of 81.63%, and
331 performance fluctuated between 81.63% and 85.71% for the remaining part of the recording. In practice,
332 this corresponds to one less or one additional correctly classified participant with respect to the full
333 recording (Fig. 3A). The knee point of the curve was identified at 5 minutes of recording length. From
334 9 minutes on, the SVM converged to an AUC of 80%. However, compared to the entire recording length
335 (AUC=88.05%), its full potential is reached from 13 minutes on (AUC robustly crossed 85%, with a
336 maximum of 89.73% at 15 minutes). The F1-score mostly overlapped with the accuracy and never
337 differed more than 0.44%. The SVM performance is plotted as a function of recording length, displayed
338 in Fig. 4A.

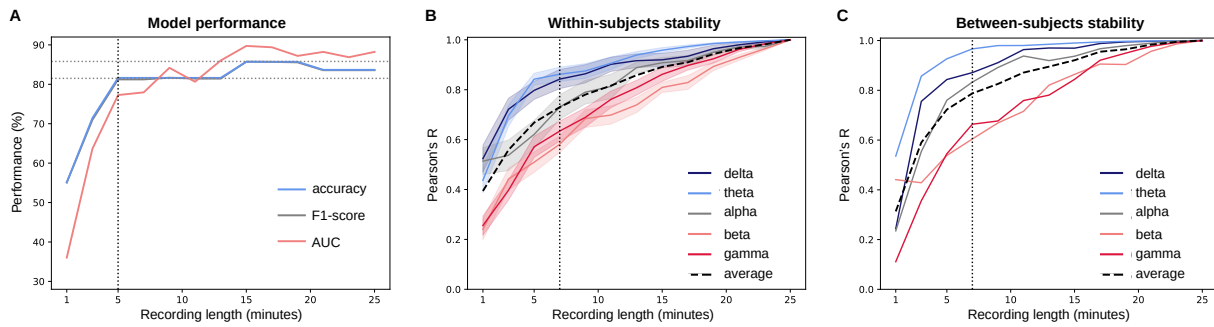


Figure 4. Recording Length. **A.** Performance (accuracy, F1-score, AUC) of the SVM classifier plotted as a function of time. **B.** Within-subjects stability for all five frequency bands and the average across frequency bands (black line). Shaded areas indicate the standard error. **C.** Between-subjects stability for all five frequency bands and the average across frequency bands (black line). The knee point of all panels is indicated with a vertical dotted line (based on the average for panels **B** and **C**).

339 The within-and between-subjects stability is plotted as a function of recording time in Fig. 4B and 4C.
 340 Highest within- and between-subjects correlations were observed for the low-frequency bands, namely
 341 delta and theta. Taking the average of all frequency bands, we identified the curve's knee point at 7
 342 minutes of recording length (see black dotted lines). The within-subjects stability (Fig. 1 4B) had an
 343 average correlation of $R=0.73$, and the between-subjects stability (Fig. 4C) had an average correlation
 344 of $R=0.79$ at the knee point of the curve.

345 3.4 Reliability of neural envelope tracking

346 Finally, we calculated the split-half reliability of neural envelope tracking. Table 1 provides the corre-
 347 lations and statistics. We generally found higher correlations in the lower frequency bands (delta and
 348 theta). Correlations were comparable between IWA and the control group; the 95% confidence intervals
 349 overlapped for each frequency band, and post-hoc Fisher z-tests, performed using the 'cocor' package
 350 in Rstudio (Diedenhofen and Musch, 2015), revealed no difference in correlation strength between both
 groups.

Table 1. Split-half reliability.

	delta		theta		alpha		beta		gamma	
	IWA	C	IWA	C	IWA	C	IWA	C	IWA	C
Pearson's R	0.85	0.91	0.96	0.92	0.75	0.88	0.61	0.62	0.62	0.73
CI	[0.68 ; 0.93]	[0.78 ; 0.96]	[0.91 ; 0.98]	[0.82 ; 0.96]	[0.52 ; 0.88]	[0.72 ; 0.95]	[0.31 ; 0.81]	[0.27 ; 0.83]	[0.31 ; 0.81]	[0.43 ; 0.88]
p-value	<0.001	<0.001	<0.001	<0.001	<0.001	<0.001	0.006	0.02	0.007	0.002
Fisher's z (p-value)	z=0.85 (1)		z=-0.94 (1)		z=1.24 (1)		z=0.04 (1)		z=0.66 (1)	

CI=95% confidence interval; C=Control group. Fisher z-test comparing controls - IWA. All p-values are corrected for multiple comparisons.

352 4 Discussion

353 We conducted an in-depth study on neural envelope tracking of natural speech in post-stroke aphasia.
354 First, we found that IWA display decreased neural envelope tracking compared to healthy controls for
355 a broadband frequency range. Second, frequency-specific analyses indicated that group differences are
356 most prominent in the delta, theta and gamma frequency ranges. Third, the suitability of neural envelope
357 tracking measures as a biomarker for post-stroke aphasia was demonstrated using an SVM classifier which
358 yielded high accuracy (84%, AUC 88%). Finally, we showed that an assessment based on neural envelope
359 tracking could be obtained in a time-efficient (5 minutes of EEG recording) and highly reliable manner.

360 4.1 Individuals with aphasia display decreased neural envelope tracking

361 Broadband frequency analysis

362 Neural envelope tracking at broadband is decreased in IWA compared to healthy controls. The single-
363 channel TMIF analysis revealed a cluster at neural response latencies centered around the second peak
364 in the TMIF comprising a large group of fronto-central, temporal and parieto-occipital channels (see
365 Fig. 1A). The multivariate TMIF confirmed this result: a temporal cluster comprising brain latencies
366 surrounding the second peak in the TMIF (Fig. 1B) was identified. A recent neural tracking study showed
367 that the second peak emerges when speech is comprehensible and diminishes when it is not understood. By
368 contrast, the first peak displayed a prominent response when speech was incomprehensible (Verschueren
369 et al., 2022). Thus, the second peak we observed here is most likely related to speech understanding,
370 while the first peak is likely more implicated in acoustically processing the signal. Therefore, it is not
371 surprising that in IWA, where language understanding is impaired, the second peak in the TMIF is
372 decreased compared to healthy controls.

373 Frequency-specific analysis

374 We further investigated neural envelope tracking in narrow frequency bands. Our findings revealed a
375 decrease in tracking for IWA compared to healthy controls in the low-frequency bands (delta and theta,
376 see Fig. 2A and 2B), which are crucial for speech understanding (Vanthornhout et al., 2018). The delta
377 band encodes sentences, phrases and words (Kaufeld et al., 2020; Keitel et al., 2018), while theta band
378 tracks the syllable rate of the stimulus (Etard and Reichenbach, 2019; Lizarazu et al., 2019). Neural
379 tracking in the low-frequency bands drops when these linguistic units become incomprehensible (Kaufeld
380 et al., 2020; Keitel et al., 2018; Xu et al., 2022). Atypical neural tracking of the low-frequency temporal
381 envelope has been reported in several clinical populations, including individuals with primary progressive
382 aphasia (Dial et al., 2021) and dyslexia (Di Liberto and Lalor, 2017; Lizarazu et al., 2021; Mandke et al.,
383 2022). In the case of dyslexia, which is characterized by phonological processing difficulties, alterations in

384 low-frequency envelope tracking are believed to reflect an atypical sampling mechanism that affects faster
385 modulations at the phoneme and grapheme level (Mandke et al., 2022). These findings in healthy and
386 clinical populations demonstrate the potential of neural tracking measures of the low-frequency envelope
387 as a biomarker for language impairments.

388 Fewer studies investigated the role of high-frequency neural envelope tracking. Some studies suggest
389 a role for alpha and beta in attention and auditory-motor coupling (Wöstmann et al., 2017; Fujioka
390 et al., 2015), and for the gamma band in encoding phonetic features (Hyafil et al., 2015; Giraud and
391 Poeppel, 2012; Gross et al., 2013). Our study found no group differences in the alpha and beta bands.
392 However, individuals with aphasia displayed decreased neural envelope tracking in the gamma band. The
393 neural response in the gamma band was characterized by an early response peak (Fig. 2) and a group
394 difference present in the right hemisphere (see Supplementary Fig. 7). This early response latency in the
395 gamma band aligns with the idea of a linear phase property, where the neural response delay in higher
396 frequency bands is shorter (Zou et al., 2021). A somewhat similar neural response pattern characterized
397 by an early response latency and a right hemisphere bias in the high gamma band (>70 Hz) was also
398 reported by Kulasingham et al. (2020). The gamma band has been of particular interest in dyslexia
399 research, with several studies reporting alterations in gamma band activity. However, most studies have
400 focused on phase-locking and phase coherence in response to amplitude-modulated noise (for a review,
401 see (Lizarazu et al., 2021)), while few have investigated gamma band neural envelope tracking during
402 natural speech processing (Mandke et al., 2022). To gain a better understanding of (low-)gamma band
403 neural envelope tracking of natural speech, which we have shown to demonstrate robust group differences
404 and contribute significantly to detecting aphasia (as depicted in Fig. 3B), future research should aim to
405 further investigate its implications for speech understanding and language impairments.

406 In line with the idea that individual frequency bands are involved in different speech processes, ex-
407 ploratory analysis revealed low to moderate positive and negative correlations between neural tracking
408 in individual frequency bands (see Supplementary Table 1). This suggests that a participant with high
409 neural tracking in one frequency band may not necessarily display high neural tracking in other frequency
410 bands. In contrast, a broadband frequency analysis shows high redundancy compared to the delta band
411 ($R=0.79$ for IWA, $R=0.92$ for controls), which can be attributed to the fact that most power in the EEG
412 and the envelope is concentrated in the lowest frequencies. This highlights the relevance of conduct-
413 ing frequency-specific analyses. We believe that the use of frequency-specific features to train the SVM
414 favored good classification results, as discussed in the next section. Future research should investigate
415 whether the neural response to these frequency bands may capture specific language deficits.

416 **4.2 High accuracy detection of post-stroke aphasia**

417 We assessed the suitability of the neural tracking technique to detect post-stroke aphasia using an SVM
418 classifier with the TMIFs computed in the individual frequency bands as input to the model. The SVM
419 robustly detected aphasia, with an accuracy of 83.67%, an F1-score of 83.58% and an AUC of 88.05%.
420 The ROC curve, plotting the true positive as a function of false positive aphasia classification, is depicted
421 in Fig. 3A. The relative contribution of individual frequency bands for detecting aphasia at the individual
422 level confirmed our group comparison results: delta, theta and gamma band neural tracking were most
423 predictive for capturing aphasia (see Fig. 3B).

424 These performance outcomes of the SVM can be interpreted against behavioral assessment. As de-
425 scribed in the Methods section, 7 out of 27 IWA (i.e., 26%) did not score below the cut-off threshold on
426 either of the two diagnostic language tests for aphasia administered during the study El Hachoui et al.
427 (2017); Van Ewijk et al. (2020). Nevertheless, these subjects had extended language deficit documen-
428 tation and followed speech-language therapy at the time of participation. Although a more extensive
429 screening for aphasia could have identified a language deficit, this finding highlights the challenge of de-
430 tecting aphasia in the chronic phase following a stroke. While further investigation is required, the higher
431 detection accuracy of the EEG-based neural tracking classification suggests that it may be more sensitive
432 than behavioral screening tests for capturing subtle language problems in individuals with aphasia.

433 Nonetheless, comparing the SVM classification accuracy to behavioral assessment is rather difficult,
434 as the underlying tested language skills are different. Standardized aphasia tests use isolated sounds,
435 phonemes, words or short sentences, questioning the ecological validity of such tasks (Hamilton and Huth,
436 2018). Consequently, research reports a discrepancy between common test outcomes and everyday life
437 speech assessments (Lesser and Algar, 1995; Kim et al., 2022; Stark et al., 2021; Wallace and Kimelman,
438 2013), and cognitive problems can bias the test result (Fonseca et al., 2019; Rohde et al., 2018). While
439 there exist behavioral natural speech assessments (Armstrong, 2000), they are only limitedly applied in
440 practice due to the high workload (time-intensive) and a lack of knowledge of natural speech analyses
441 (Bryant et al., 2019; Stark et al., 2021). Novel automatic speech recognition and natural language
442 processing techniques (Dalton et al., 2022; Jamal et al., 2017; Le et al., 2018) may provide a solution in
443 the future. The neural tracking technique directly addresses the limitation of low ecological validity from
444 which behavioral tests suffer.

445 **4.3 Assessing time-efficiency, stability and reliability**

446 We investigated how much data neural envelope tracking requires to detect aphasia accurately and yield
447 reliable results. We assessed SVM classification performance as a function of recording time, as shown
448 in Fig. 4A. Our findings indicate that high-accuracy detection can be achieved with just 5 minutes
449 of recording time (accuracy of 81.63%). However, extending the recording duration to 13 minutes can

450 provide additional benefits in terms of the AUC, with a robust increase above 85%, and a maximum AUC
451 of 89.73% achieved at 15 minutes. In summary, our results demonstrate that neural envelope tracking
452 can effectively detect aphasia in a time-efficient manner, consistent with prior recommendations that
453 language assessments in aphasia should not exceed 15 minutes to avoid fatigue and cognitive/attentional
454 challenges (El Hachoui et al., 2014). Our findings have important implications for potential clinical
455 applications of neural envelope tracking in aphasia.

456 We further investigated the amount of data necessary for our frequency band features to achieve
457 stability. Our within- and between-subjects stability analysis revealed that 7 minutes recording length is
458 sufficient for the TMIF of individual subjects and at the group-level to resemble the TMIF from the entire
459 recording (see Fig. 4B and 4C). These findings were consistent within both groups, with 7 minutes being
460 the minimum recording length required (as illustrated in Supplementary Fig. 8). Notably, we observed
461 that lower frequency bands (delta and theta) converge more rapidly compared to higher frequency bands.
462 Within 3-5 minutes, stability correlations for these bands were relatively high, robustly crossing $R=0.80$.
463 In contrast, higher frequency bands require a longer time to converge and exhibit a more linear slope
464 compared to the delta and theta bands. These less stable results and longer minimal recording length
465 for the higher frequency bands can be attributed to their lower signal-to-noise ratio.

466 To summarize, our results indicate that 5-7 minutes of recording time are sufficient for assessing neu-
467 ral envelope tracking at low-frequency ranges, which reflect higher-level linguistic processes and speech
468 understanding. However, a more comprehensive evaluation that includes higher frequency bands, which
469 can provide minor additional benefits, requires a slightly longer recording duration (>13 minutes). These
470 findings are consistent with previous research in healthy participants, which suggests that low-frequency
471 neural tracking requires approximately 3-10 minutes of recording time for robust outcomes (Desai et al.,
472 2023; Di Liberto and Lalor, 2017; Mesik and Wojtczak, 2022). Our study contributes an innovative
473 approach by defining the minimal recording length required to detect language impairments at the in-
474 dividual level and suggests that the recording duration for future studies in individuals with language
475 impairments may depend on the specific research question being addressed.

476 Previous studies on aphasia using ERPs have suggested the potential of this approach for clinical diag-
477 nosis, but without reporting on its reliability (Cocquyt et al., 2020). However, evaluating the reliability
478 of test results is crucial to determine the usefulness of capturing individual language impairments. In
479 this study, we assessed the reliability of neural envelope tracking using split-half reliability metrics. The
480 results demonstrate strong correlations between both halves, particularly in the delta and theta bands
481 (Table 1). Our findings are consistent with previous research reporting a correlation of $R=0.89$ for delta
482 and $R=0.82$ for theta across two stories in a cohort with language impairments caused by a neurode-
483 generative disorder (Dial et al., 2021). Yet, reliability measures in our study were generally lower for
484 higher frequency bands. As mentioned earlier, these bands require more data to converge and have a

485 lower signal-to-noise ratio. It is worth noting that our reliability measure may be affected by fatigue.
486 Thus, future studies should examine the generalizability of the results across stories and speakers at
487 different sessions (i.e., test-retest) to further investigate the reliability of neural tracking for applications
488 in aphasia.

489 **4.4 Limitations and future directions**

490 Our study demonstrates that neural envelope tracking is a reliable and accurate method for detecting
491 language impairments in aphasia. However, our current approach does not provide information on the
492 specific language profile of the patient (i.e., which underlying language component, e.g., auditory, pho-
493 netic, semantic,... is affected). Investigating these deficits would require a larger sample size with a
494 more uniform spread of aphasia severity levels. In future research, we suggest exploring whether neural
495 tracking in specific frequency bands can cluster different language profiles in aphasia. In addition, recent
496 studies investigated the neural response to speech representations beyond the temporal envelope. For
497 example, it has been shown that linguistic speech representations at phoneme and word level can improve
498 the model's fit to the EEG (Di Liberto et al., 2015; Gillis et al., 2021) and can provide complementary
499 information on speech processing (Verschueren et al., 2022; Gillis, Kries et al., 2023). Future research
500 should (1) examine whether incorporating these linguistic speech representations can enhance aphasia
501 detection and inform on specific language deficits and (2) assess the reliability and robustness of these
502 features, which is currently lacking in the literature.

503 Several other open questions must be addressed before neural tracking can be applied in clinical settings.
504 Firstly, neural tracking must be applied to IWA in the acute stage after stroke. This work considered
505 the chronic stage only since it is characterized by a more stable language profile (Johnson et al., 2019).
506 Secondly, the present study distinguished IWA and healthy controls only. If neural tracking is to be
507 used for screening aphasia in the acute stage post-stroke, a clear dissociation between stroke patients
508 with and without aphasia is crucial. However, such dissociation is generally not considered in behavioral
509 screening tests despite being used in the clinic on a daily basis (Rohde et al., 2018). Lastly, this study
510 used language stimuli in the receptive domain only. Recent studies have suggested that the same analysis
511 can also be applied to the expressive domain, i.e., speech production (Perez et al., 2022), which could
512 open new perspectives to studying expressive language problems in IWA.

513 **Conclusion**

514 This study investigated neural envelope tracking of natural speech in patients with chronic post-stroke
515 aphasia. The findings showed that individuals with aphasia exhibited reduced brain responses in the
516 delta, theta, and gamma bands, likely reflecting decreased processing of higher-level auditory and linguis-
517 tic units. The study also demonstrated the efficacy of neural tracking in capturing language impairments

518 at the individual level in a highly reliable and time-efficient manner, which suggests its promising clinical
519 potential as an assessment tool. Despite these positive results, several open questions remain that need
520 to be addressed before neural tracking can be used in clinical settings. For instance, it remains un-
521 clear whether neural tracking can accurately capture specific language problems, and its effectiveness in
522 assessing patients in the acute stage post-stroke requires future investigation. Nevertheless, our work rep-
523 resents a significant step towards more automatic and ecologically valid assessments of language problems
524 in aphasia.

525 **Acknowledgements**

526 The authors would like to express their heartfelt gratitude to all the participants, particularly those with
527 aphasia and their families that supported them. We would also like to extend our thanks to Dr. Klara
528 Schevenels for her assistance in the recruitment process, as well as the individuals that helped with the
529 data collection: Janne Segers, Rosanne Partoens, Charlotte Rommel, Ines Robberechts, Laura Van Den
530 Bergh, Anke Heremans, Frauke De Vis, Mouna Vanlommel, Naomi Pollet, Kaat Schroeven, Pia Reynaert
531 and Merel Dillen.

532 **Funding**

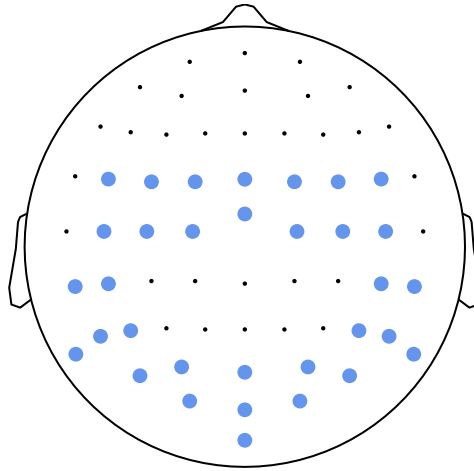
533 Research of Pieter De Clercq was supported by the Research Foundation Flanders (FWO; PhD grant
534 1S40122N). Jill Kries was financially supported by the Luxembourg National Research Fund (FNR; AFR-
535 PhD project reference 13513810). Research of Jonas Vanthornhout was supported by FWO (postdoctoral
536 grant: 1290821N). The presented study further received funding from the European Research Council
537 (ERC) under the European Union's Horizon 2020 research and innovation programme (Tom Francart;
538 grant agreement No. 637424), and by the FWO grant No. G0D8520N.

539 **Competing interests**

540 The authors declare no conflicts of interest, financial or otherwise.

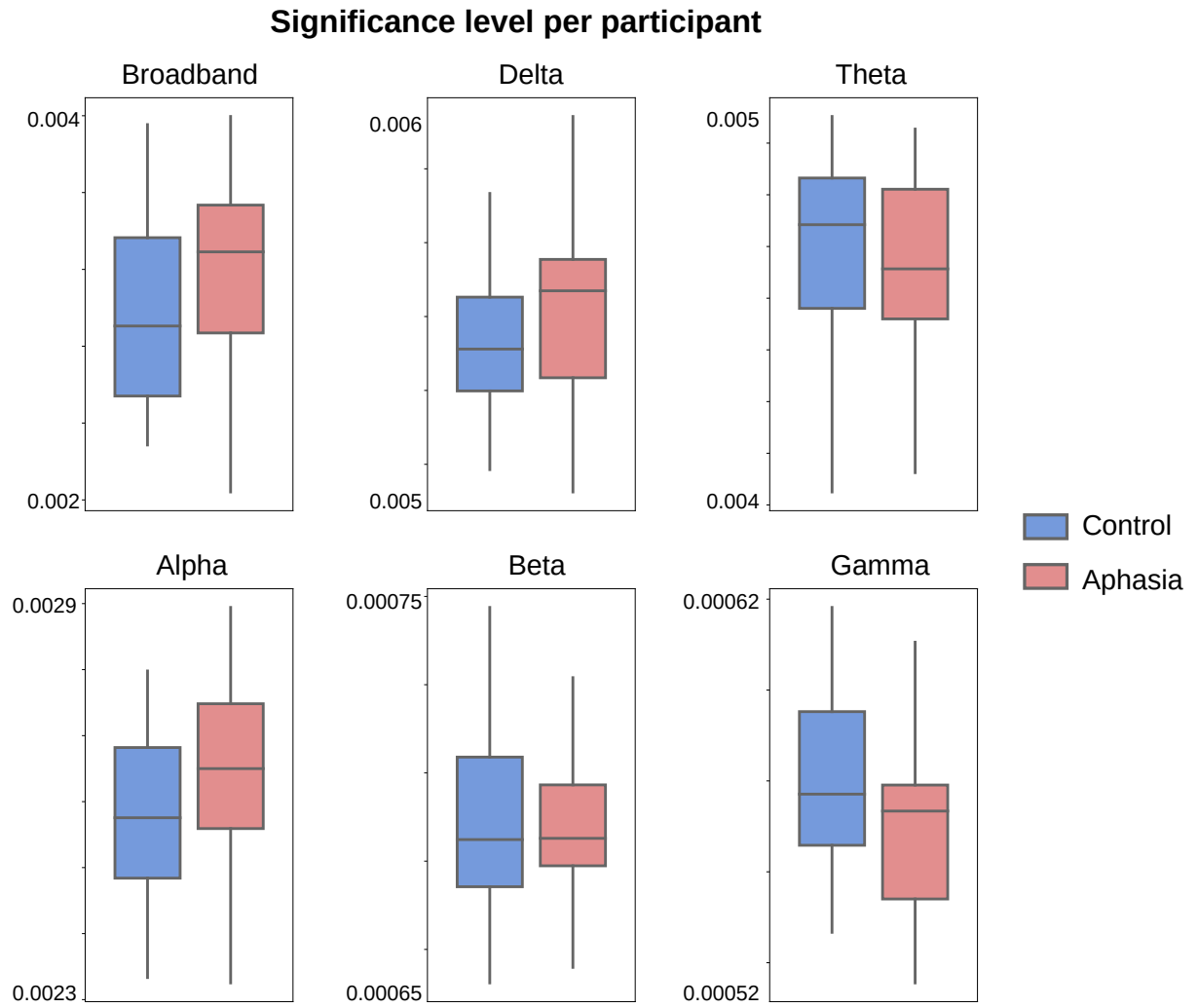
541 **Supplementary material**

542 **Channel Selection**



Supplementary Fig. 1. Channel selection.

543 **Significance level of neural envelope tracking**

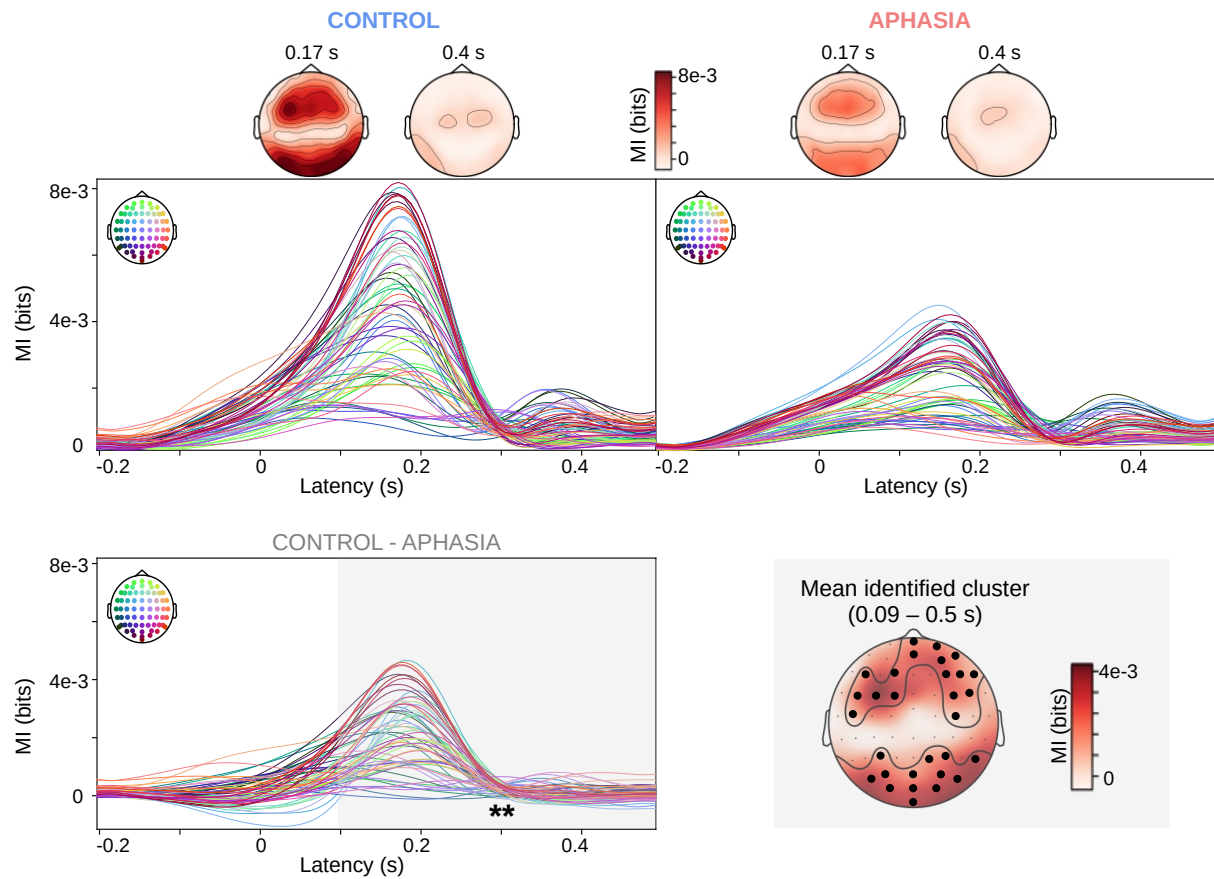


Supplementary Fig. 2. Significance level of neural tracking. Boxes represent the 95th percentile of permutations per subject and per frequency band. There was no significant difference between groups for any frequency band.

544 **Single-channel TMIF analysis**

545 **Delta band**

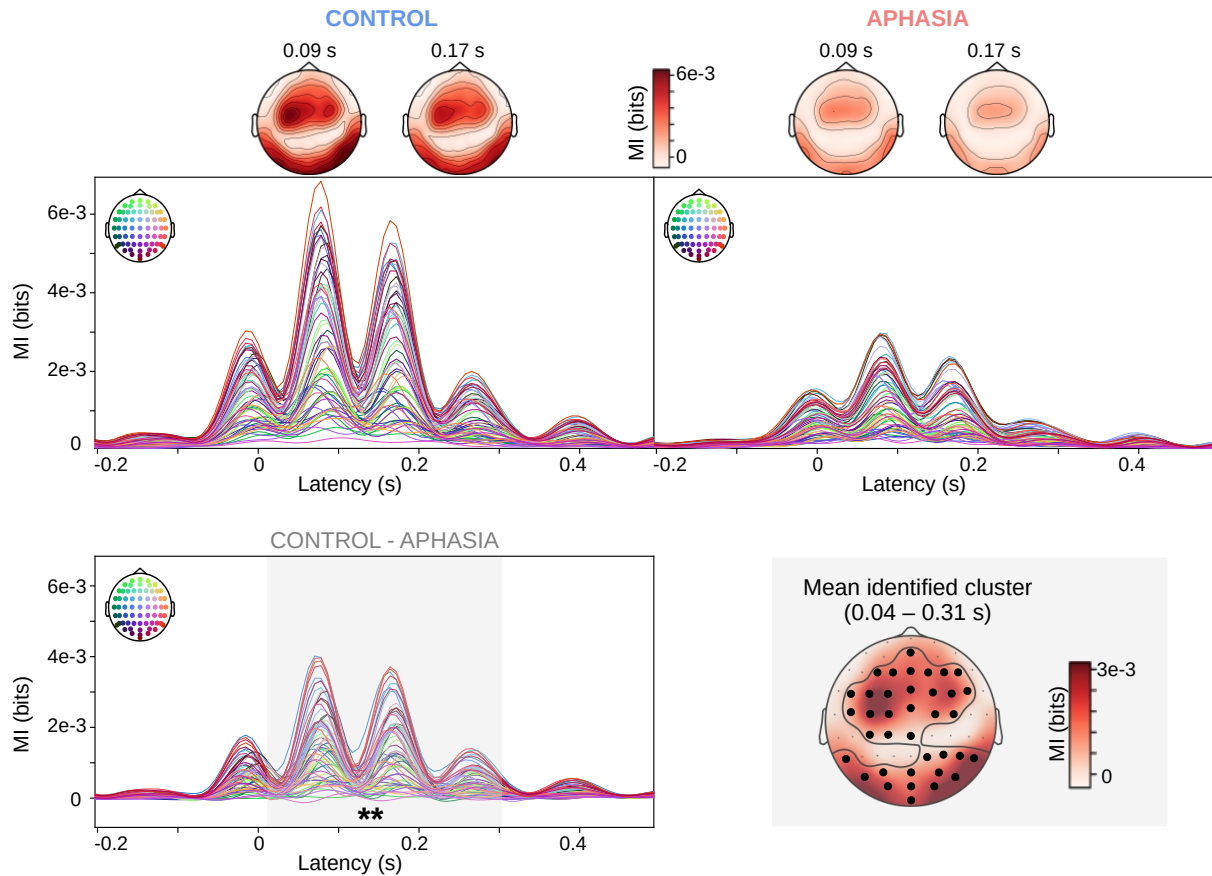
546 The single-channel TMIF analysis revealed decreased delta band envelope tracking for IWA compared
547 to healthy controls. A spatio-temporal cluster-based permutation test identified a cluster ($p=0.005$)
548 comprising a large group of bilateral fronto-central, parietal and posterior channels ($N = 46$ channels)
549 and brain latencies from 0.09 s to 0.5 s. The results are depicted in Fig. 3.



Supplementary Fig. 3. Delta band analysis. The average single-channel TMIF in delta band for the control and the aphasia group separately, with topoplots at indicated brain latencies. The spatio-temporal cluster-based permutation test investigated the difference between the control and aphasia group (control - aphasia) and identified a cluster (below threshold $p<0.05$) with the largest group difference. Brain latencies belonging to the cluster are marked in a shaded gray area, the channels belonging to the cluster are indicated with a black dot on the topoplot. ** = $p<0.01$

550 **Theta band**

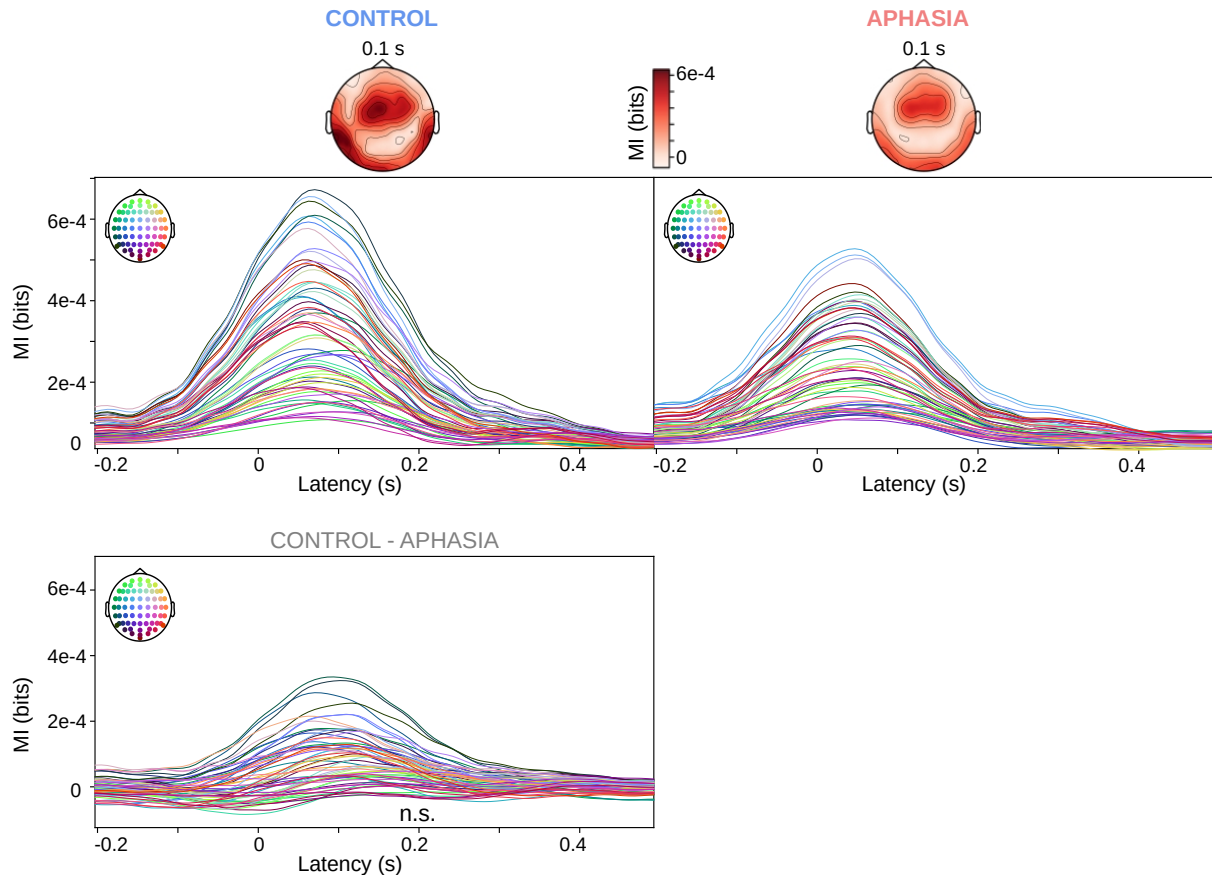
551 For the theta band, the single-channel TMIF analysis revealed decreased envelope tracking for IWA
552 compared to healthy controls. A spatio-temporal cluster-based permutation test identified a cluster
553 ($p=0.005$) comprising a large group of bilateral fronto-central, parietal and posterior channels ($N = 40$
554 channels) and brain latencies from 0.09 s to 0.31 s. Fig. 4 visualizes the result.



Supplementary Fig. 4. Theta band analysis. The average single-channel TMIF in theta band for the control and the aphasia group separately, with topoplots at indicated brain latencies. The spatio-temporal cluster-based permutation test investigated the difference between the control and aphasia group (control - aphasia) and identified a cluster (below threshold $p < 0.05$) with the largest group difference. Brain latencies belonging to the cluster are marked in a shaded gray area, the channels belonging to the cluster are indicated with a black dot on the topoplot. ** = $p < 0.01$

555 **Alpha band**

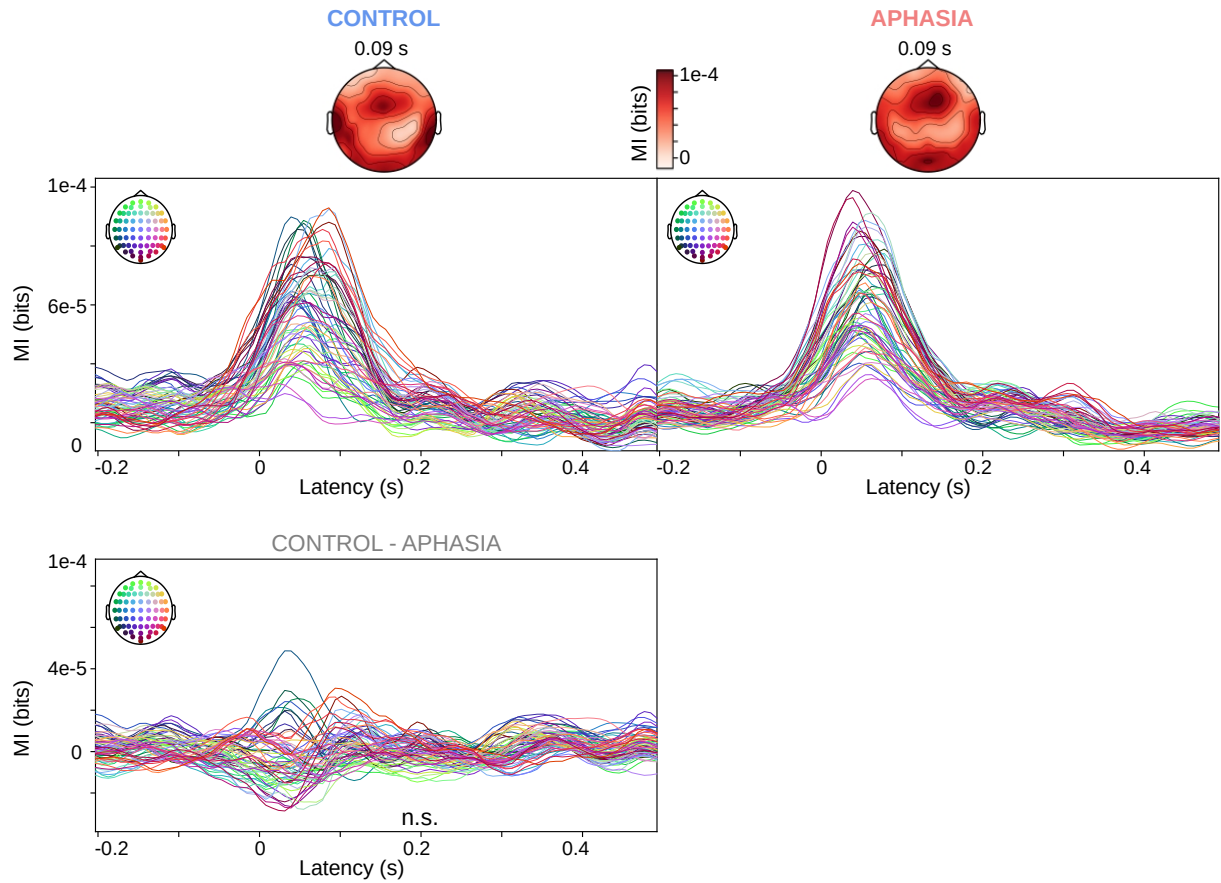
556 In the alpha band, a spatio-temporal cluster-based permutation test found no clusters exceeding $p < 0.05$
557 threshold level. The group results are displayed in Fig. 5.



Supplementary Fig. 5. Alpha band analysis. The average single-channel TMIF in alpha band for the control and the aphasia group separately, with topoplots at indicated brain latencies. The spatio-temporal cluster-based permutation test investigated the difference between the control and aphasia group (control - aphasia), but did not find a group difference with p-value below threshold level 0.05.

558 **Beta band**

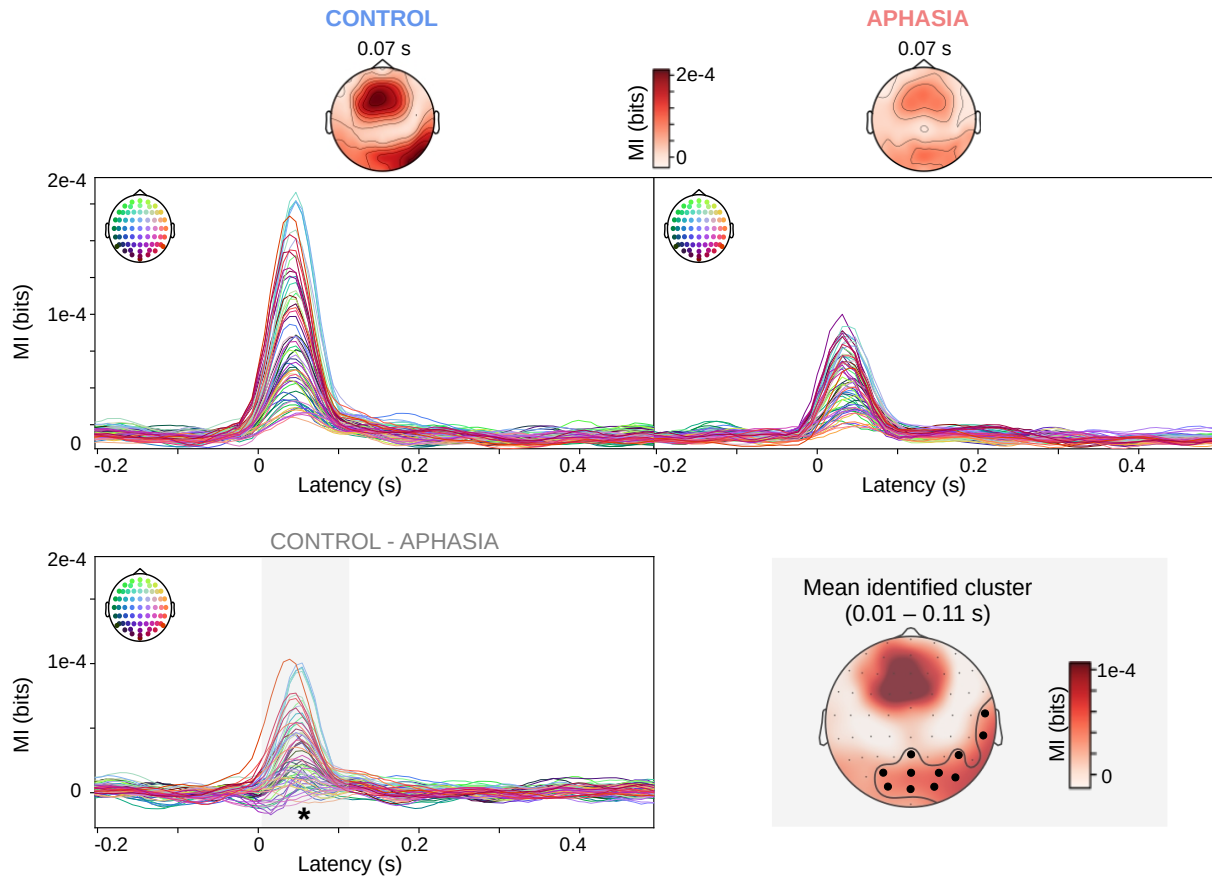
559 In the beta band, a spatio-temporal cluster-based permutation test found no clusters exceeding $p < 0.05$
560 threshold level. The group results are displayed in Fig. 6.



Supplementary Fig. 6. Beta band analysis. The average single-channel TMIF in beta band for the control and the aphasia group separately, with topoplots at indicated brain latencies. The spatio-temporal cluster-based permutation test investigated the difference between the control and aphasia group (control - aphasia), but did not find a group difference with p -value below threshold level 0.05.

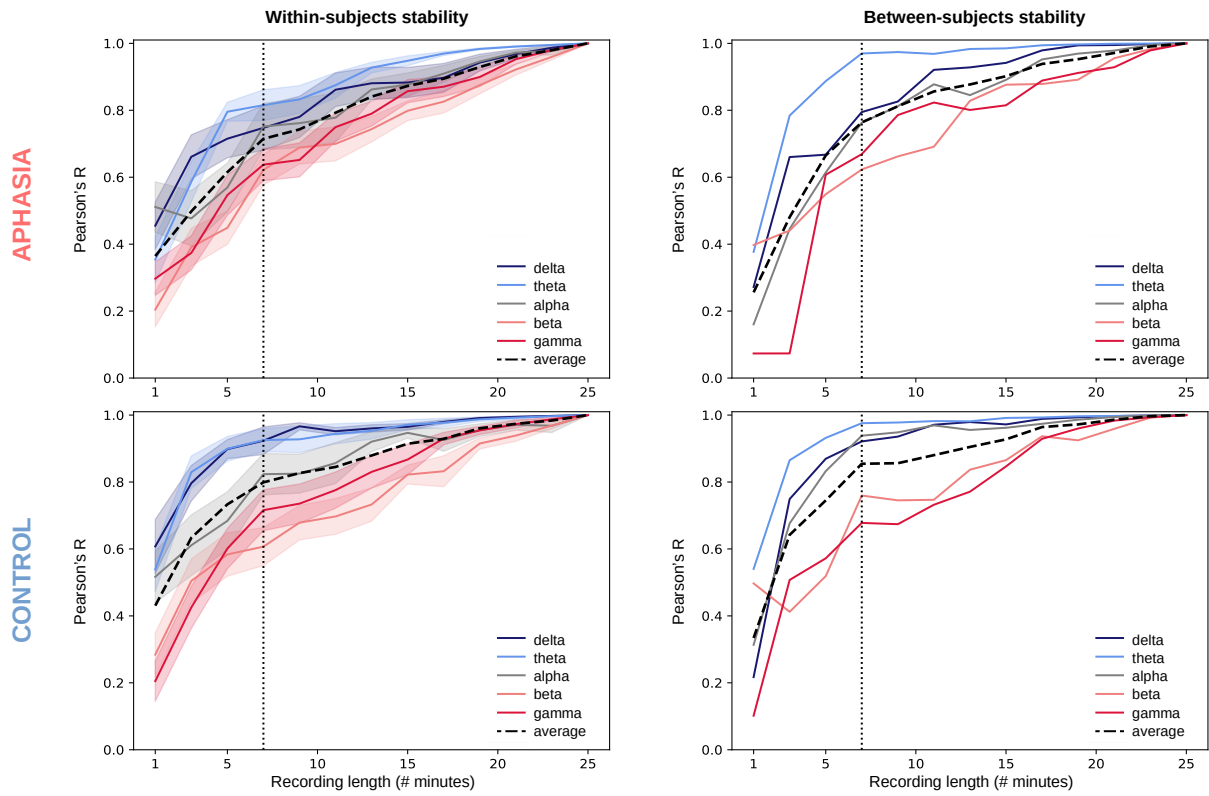
561 **Gamma band**

562 Finally, IWA displayed decreased neural envelope tracking in the gamma band. A spatio-temporal cluster-
563 based permutation test identified a cluster ($p=0.03$) comprising parietal and posterior channels ($N = 12$
564 channels), primarily in the right hemisphere, and brain latencies from 0.01 s to 0.11 s. Fig. 7 visualizes
565 the result.



Supplementary Fig. 7. Gamma band analysis. The average single-channel TMIF in gamma band for the control and the aphasia group separately, with topoplots at indicated brain latencies. The spatio-temporal cluster-based permutation test investigated the difference between the control and aphasia group (control - aphasia) and identified a cluster (below threshold $p < 0.05$) with the largest group difference. Brain latencies belonging to the cluster are marked in a shaded gray area, the channels belonging to the cluster are indicated with a black dot on the topoplots. * = $p < 0.05$

566 Group-specific stability analysis



Supplementary Fig. 8. Stability measures grouped. Within- and between-subjects stability analysis performed for each group separately. Black dotted line indicates the average across frequencies. Shaded areas indicate the standard error of the correlations. The knee point of all panels is indicated with a vertical dotted line (based on the average across frequencies)

567 **Correlation matrix frequency bands**

Supplementary Table 1. Correlation matrix neural envelope tracking

	IWA						Controls					
	broad	delta	theta	alpha	beta	gamma	broad	delta	theta	alpha	beta	gamma
broad	1						1					
delta	0.79	1					0.92	1				
theta	0.15	0.01	1				0.09	0.02	1			
alpha	0.15	0.07	0.71	1			0.27	0.15	0.52	1		
beta	0.15	0.20	0.62	0.61	1		0.48	0.57	0.32	0.44	1	
gamma	0.19	0.22	-0.01	0.01	0.23	1	0.12	0.18	-0.18	-0.22	0.26	1

Exploratory analysis investigating the collinearity between frequency bands. The table displays the Pearson correlations for the mean MI (integration window 0-400 ms).

References

- 568
- 569 Aerts, A., van Mierlo, P., Hartsuiker, R. J., Santens, P., and Letter, M. D. (2015). Neurophysiological
570 sensitivity for impaired phonological processing in the acute stage of aphasia. *Brain and Language*,
571 149:84–96.
- 572 Armstrong, E. (2000). Aphasic discourse analysis: The story so far. *Aphasiology*, 14(9):875–892.
- 573 Becker, F. and Reinvang, I. (2007). Successful syllable detection in aphasia despite processing impairments
574 as revealed by event-related potentials. *Behavioral and Brain Functions*, 3.
- 575 Brodbeck, C., Das, P., Gillis, M., Kulasingham, J. P., Bhattasali, S., Gaston, P., Resnik, P., and Simon,
576 J. Z. (2022). Eelbrain: A python toolkit for time-continuous analysis with temporal response functions.
577 *bioRxiv*.
- 578 Bryant, L., Ferguson, A., Valentine, M., and Spencer, E. (2019). Implementation of discourse analysis in
579 aphasia: investigating the feasibility of a knowledge-to-action intervention. *Aphasiology*, 33(1):31–57.
- 580 Cocquyt, E. M., Vandewiele, M., Bonnarens, C., Santens, P., and De Letter, M. (2020). The sensitivity of
581 event-related potentials/fields to logopedic interventions in patients with stroke-related aphasia. *Acta*
582 *neurologica Belgica*, 120(4):805–817.
- 583 Crosse, M. J., Zuk, N. J., Di Liberto, G. M., Nidiffer, A. R., Molholm, S., and Lalor, E. C. (2021).
584 Linear modeling of neurophysiological responses to speech and other continuous stimuli: Methodological
585 considerations for applied research. *Frontiers in Neuroscience*, 15.
- 586 Dalton, S. G., Stark, B. C., Fromm, D., Apple, K., MacWhinney, B., Rensch, A., and Rowedder, M.
587 (2022). Validation of an automated procedure for calculating core lexicon from transcripts. *Journal of*
588 *Speech, Language, and Hearing Research*, 65(8):2996–3003.
- 589 De Clercq, P., Vanthornhout, J., Vandermosten, M., and Francart, T. (2023). Beyond linear neural
590 envelope tracking: a mutual information approach. *Journal of Neural Engineering*, 20(2):026007.
- 591 de Renzi, E. and Ferrai, C. (1978). The reporter’s test: A sensitive test to detect expressive disturbances
592 in aphasics. *Cortex*, 14(2):279–293.
- 593 Decruy, L., Vanthornhout, J., and Francart, T. (2019). Evidence for enhanced neural tracking of
594 the speech envelope underlying age-related speech-in-noise difficulties. *Journal of Neurophysiology*,
595 122(2):601–615.
- 596 Desai, M., Field, A. M., and Hamilton, L. S. (2023). Dataset size considerations for robust acoustic and
597 phonetic speech encoding models in eeg. *Frontiers in Human Neuroscience*, 16.

- 598 Devanga, S. R., Pollens, R. D., and Glista, S. O. (2021). Toward developing outcome measures in
599 university-based aphasia programs: Perspectives from the aphasia communication enhancement pro-
600 gram. *Perspectives of the ASHA Special Interest Groups*, 6(5):1047–1059.
- 601 Di Liberto, G. M. and Lalor, E. C. (2017). Indexing cortical entrainment to natural speech at the
602 phonemic level: Methodological considerations for applied research. *Hearing Research*, 348:70–77.
- 603 Di Liberto, G. M., O’Sullivan, J. A., and Lalor, E. C. (2015). Low-frequency cortical entrainment to
604 speech reflects phoneme-level processing. *Current Biology*, 25(19):2457–2465.
- 605 Dial, H. R., Gnanateja, G. N., Tessmer, R. S., Gorno-Tempini, M. L., Chandrasekaran, B., and Henry,
606 M. L. (2021). Cortical tracking of the speech envelope in logopenic variant primary progressive aphasia.
607 *Frontiers in Human Neuroscience*, 14.
- 608 Diedenhofen, B. and Musch, J. (2015). cocor: a comprehensive solution for the statistical comparison of
609 correlations. *PLoS ONE*, 10(3):e0121945.
- 610 Ding, N., Melloni, L., Zhang, H., Tian, X., and Poeppel, D. (2016). Cortical tracking of hierarchical
611 linguistic structures in connected speech. *Nat. Neurosci.*, 19:158–164.
- 612 Ding, N. and Simon, J. Z. (2013). Adaptive temporal encoding leads to a background-insensitive cortical
613 representation of speech. *Journal of Neuroscience*, 33(13):5728–5735.
- 614 El Hachoui, H., Visch-Brink, E. G., de Lau, L. M., van de Sandt-Koenderman, M. W., Nouwens, F.,
615 Koudstaal, P. J., and Dippel, D. W. (2017). Screening tests for aphasia in patients with stroke: a
616 systematic review. *Journal of Neurology*, 264(2):211–220.
- 617 El Hachoui, H., Visch-Brink, E. G., Lingsma, H. F., Van De Sandt-Koenderman, M. W., Dippel, D. W.,
618 Koudstaal, P. J., and Middelkoop, H. A. (2014). Nonlinguistic cognitive impairment in poststroke
619 aphasia: A prospective study. *Neurorehabilitation and Neural Repair*, 28(3):273–281.
- 620 Etard, O. and Reichenbach, T. (2019). Neural speech tracking in the theta and in the delta frequency
621 band differentially encode clarity and comprehension of speech in noise. *Journal of Neuroscience*,
622 39(29):5750–5759.
- 623 Fonseca, J., Raposo, A., and Martins, I. P. (2019). Cognitive functioning in chronic post-stroke aphasia.
624 *Applied Neuropsychology: Adult*, 26(4):355–364.
- 625 Francart, T., Wieringen, A. V., and Wouters, J. (2008). Apex 3: a multi-purpose test platform for
626 auditory psychophysical experiments. *J Neurosci Methods*, 172:283–293.
- 627 Fujioka, T., Ross, B., and Trainor, L. J. (2015). Beta-band oscillations represent auditory beat and its
628 metrical hierarchy in perception and imagery. *Journal of Neuroscience*, 35(45):15187–15198.

- 629 Gillis, M., Van Canneyt, J., Francart, T., and Vanthornhout, J. (2022). Neural tracking as a diagnostic
630 tool to assess the auditory pathway. *Hearing Research*, page 108607.
- 631 Gillis, M., Vanthornhout, J., Simon, J. Z., Francart, T., and Brodbeck, C. (2021). Neural markers of
632 speech comprehension: Measuring eeg tracking of linguistic speech representations, controlling the
633 speech acoustics. *The Journal of Neuroscience*, 41(50):10316–10329.
- 634 Gillis, Kries, Vandermosten, M., and Francart, T. (2023). Neural tracking of linguistic and acoustic
635 speech representations decreases with advancing age. *NeuroImage*, 267(119841):1–16.
- 636 Giraud, A. and Poeppel, D. (2012). Cortical oscillations and speech processing: emerging computational
637 principles and operations. *Nat. Neurosci.*, 15:511–517.
- 638 Gross, J., Hoogenboom, N., Thut, G., Schyns, P., Panzeri, S., Belin, P., and Garrod, S. (2013). Speech
639 rhythms and multiplexed oscillatory sensory coding in the human brain. *PLoS Biology*, 11(12):e1001752.
- 640 Hamilton, L. S. and Huth, A. G. (2018). The revolution will not be controlled: natural stimuli in speech
641 neuroscience. *Language, cognition and neuroscience*, 35(5):573–582.
- 642 Hyafil, A., Giraud, A.-L., Fontolan, L., and Gutkin, B. (2015). Neural cross-frequency coupling: Con-
643 necting architectures, mechanisms, and functions. *Trends in Neurosciences*, 38(11):725–740.
- 644 Ilvonen, T. M., Kujala, T., Tervaniemi, M., Salonen, O., Näätänen, R., and Pekkonen, E. (2001). The pro-
645 cessing of sound duration after left hemisphere stroke: Event-related potential and behavioral evidence.
646 *Psychophysiology*, 38:622–628.
- 647 Ince, R. A. A., Giordano, B., Kayser, C., Rousselet, G., Gross, J., and Schyns, P. (2017). A statistical
648 framework for neuroimaging data analysis based on mutual information estimated via a gaussian copula.
649 *Human brain mapping*, 38(3):1541–1573.
- 650 Jamal, N., Shanta, S., Mahmud, F., and Sha’abani, M. (2017). Automatic speech recognition (asr)
651 based approach for speech therapy of aphasic patients: A review. *AIP Conference Proceedings*,
652 1883(1):020028.
- 653 Jansen, S., Luts, H., Wagener, K. C., Kollmeier, B., Del Rio, M., Dauman, R., James, C., Fraysse, B.,
654 Vormès, E., Frachet, B., Wouters, J., and van Wieringen, A. (2012). Comparison of three types of
655 french speech-in-noise tests: A multi-center study. *International Journal of Audiology*, 51(3):164–173.
- 656 Johnson, L., Basilakos, A., Yourganov, G., Cai, B., Bonilha, L., Rorden, C., and Fridriksson, J. (2019).
657 Progression of aphasia severity in the chronic stages of stroke. *American Journal of Speech-Language*
658 *Pathology*, 28(2):639–649.

- 659 Kandylaki, K. D. and Bornkessel-Schlesewsky, I. (2019). From story comprehension to the neurobiology
660 of language. *Language, Cognition and Neuroscience*, 34(4):405–410.
- 661 Kaufeld, G., Bosker, H. R., Alday, P. M., Meyer, A. S., and Martin, A. E. (2020). Linguistic structure
662 and meaning organize neural oscillations into a content-specific hierarchy. *Journal of Neuroscience*,
663 40(49):9467–9475.
- 664 Keitel, A., Gross, J., and Kayser, C. (2018). Perceptually relevant speech tracking in auditory and motor
665 cortex reflects distinct linguistic features. *PLoS Biology*, 16(3):e2004473.
- 666 Kertesz, A. (1982). Western aphasia battery. *New York: Grune and Stratton*.
- 667 Kim, H., Berube, S., and Hillis, A. E. (2022). Core lexicon in aphasia: A longitudinal study. *Aphasiology*,
668 0(0):1–13.
- 669 Kries, J., De Clercq, P., Lemmens, R., Francart, T., and Vandermosten, M. (2022). Tuning in on auditory
670 details is difficult: Individuals with aphasia show impaired acoustic and phonemic processing. *bioRxiv*.
- 671 Kulasingham, J. P., Brodbeck, C., Presacco, A., Kuchinsky, S. E., Anderson, S., and Simon, J. Z. (2020).
672 High gamma cortical processing of continuous speech in younger and older listeners. *NeuroImage*,
673 222:117291.
- 674 Lalor, E. C., Power, A. J., Reilly, R. B., and Foxe, J. J. (2009). Resolving precise temporal processing
675 properties of the auditory system using continuous stimuli. *Journal of Neurophysiology*, 102(1):349–359.
- 676 Le, D., Licata, K., and Mower Provost, E. (2018). Automatic quantitative analysis of spontaneous aphasic
677 speech. *Speech Communication*, 100:1–12.
- 678 Lesenfants, D., Vanthornhout, J., Verschueren, E., Decruy, L., and Francart, T. (2019). Predicting
679 individual speech intelligibility from the neural tracking of acoustic- and phonetic-level speech repre-
680 sentations. *Hearing Research*, 380:1–9.
- 681 Lesser, R. and Algar, L. (1995). Towards combining the cognitive neuropsychological and the pragmatic
682 in aphasia therapy. *Neuropsychological Rehabilitation*, 5(1-2):67–92.
- 683 Lizarazu, M., Lallier, M., Bourguignon, M., Carreiras, M., and Molinaro, N. (2021). Impaired neural
684 response to speech edges in dyslexia. *Cortex*, 135:207–218.
- 685 Lizarazu, M., Lallier, M., and Molinaro, N. (2019). Phase amplitude coupling between theta and gamma
686 oscillations adapts to speech rate. *Annals of the New York Academy of Sciences*, 1453(1):140–152.
- 687 Mandke, K., Flanagan, S., Macfarlane, A., Gabrielczyk, F., Wilson, A., Gross, J., and Goswami, U.
688 (2022). Neural sampling of the speech signal at different timescales by children with dyslexia. *Neu-
689 roImage*, 253:119077.

- 690 Maris, E. and Oostenveld, R. (2007). Nonparametric statistical testing of eeg- and meg-data. *Journal of*
691 *Neuroscience Methods*, 164(1):177–190.
- 692 Mesik, J. and Wojtczak, M. (2022). The effects of data quantity on performance of temporal response
693 function analyses of natural speech processing. *bioRxiv*.
- 694 Mullen, T. R., Kothe, C. A. E., Chi, Y. M., Ojeda, A., Kerth, T., Makeig, S., Jung, T. P., and Cauwen-
695 bergs, G. (2015). Real-time neuroimaging and cognitive monitoring using wearable dry eeg. *IEEE*
696 *Transactions on Biomedical Engineering*, 11(62):2553–2567.
- 697 Ofek, E., Purdy, S. C., Ali, G., Webster, T., Gharahdaghi, N., and McCann, C. M. (2013). Processing of
698 emotional words after stroke: An electrophysiological study. *Clinical Neurophysiology*, 124:1771–1778.
- 699 Papathanasiou, I. and Coppens, P. (2017). Aphasia and related neurogenic communication disorders.
700 *Burlington, MA: Jones and Bartlett Learning*.
- 701 Pedregosa, F., Varoquaux, G., Gramfort, A., Michel, V., Thirion, B., Grisel, O., Blondel, M., Pretten-
702 hofer, P., Weiss, R., Dubourg, V., Vanderplas, J., Passos, A., Cournapeau, D., Brucher, M., Perrot,
703 M., and Duchesnay, E. (2011). Scikit-learn: Machine learning in python. *J. Mach. Learn. Res.*,
704 12:2825–2830.
- 705 Pedroni, A., Bahreini, A., and Langer, N. (2019). Automagic: Standardized preprocessing of big eeg
706 data. *NeuroImage*, 200(null):460–473.
- 707 Peelle, J. E. and Davis, M. H. (2012). Neural oscillations carry speech rhythm through to comprehension.
708 *Front Psychol*, 3.
- 709 Perez, A., Davis, M. H., Ince, R. A. A., Zhang, H., Zhanao, F., Lamarca, M., Lambon Ralph, M. A., and
710 Monahan, P. J. (2022). Timing of brain entrainment to the speech envelope during speaking, listening
711 and self-listening. *Cognition*, 224:105051.
- 712 Pion-Tonachini, L., Kreutz-Delgado, K., and Makeig, S. (2019). Iclabel: An automated electroencephalo-
713 graphic independent component classifier, dataset, and website. *NeuroImage*, 198(null):181–197.
- 714 Pulvermüller, F., Mohr, B., and Lutzenberger, W. (2004). Neurophysiological correlates of word and
715 pseudo-word processing in well-recovered aphasics and patients with right hemispheric stroke. *Psy-*
716 *chophysiology*, 41:584–591.
- 717 Robson, H., Pilkington, E., Evans, L., DeLuca, V., and Keidel, J. L. (2017). Phonological and semantic
718 processing during comprehension in Wernicke’s aphasia: An N400 and Phonological Mapping Negativ-
719 ity Study. *Neuropsychologia*, 100(October 2016):144–154.

- 720 Rohde, A., Worrall, L., Godecke, E., O'Halloran, R., Farrell, A., and Massey, M. (2018). Diagnosis of
721 aphasia in stroke populations: A systematic review of language tests. *PLoS ONE*, 13(3):e0194143.
- 722 Satopaa, V., Albrecht, J., Irwin, D., and Raghavan, B. (2011). Finding a "kneedle" in a haystack: De-
723 tecting knee points in system behavior. *2011 31st International Conference on Distributed Computing*
724 *Systems Workshops*, pages 166–171.
- 725 Shannon, R. V., Zeng, F. G., V, K., Wygonski, J., and S, E. M. (1995). Speech recognition with primarily
726 temporal cues. *Science*, 270(5234):303–304.
- 727 Stark, B. C., Dutta, M., Murray, L. L., Fromm, D., Bryant, L., Harmon, T. G., Ramage, A. E., and
728 Roberts, A. C. (2021). Spoken discourse assessment and analysis in aphasia: An international survey
729 of current practices. *Journal of Speech, Language, and Hearing Research*, 64(11):4366–4389.
- 730 Søndergaard, P., Torrèsani, B., and Balazs, P. (2012). The linear time frequency analysis toolbox.
731 *International Journal of Wavelets Multiresolution and Information Processing*, 10:1250032.
- 732 Van Ewijk, E., Dijkhuis, L., Hofs-Van Kats, M., Hendrickx-Jessurun, M., Wijngaarden, M., and De
733 Hilster, C. (2020). *Nederlandse Benoem Test*. Bohn stafleu van loghum.
- 734 Vanthornhout, J., Decruy, L., Wouters, J., Simon, J. Z., and Francart, T. (2018). Speech intelligibility
735 predicted from neural entrainment of the speech envelope. *JARO - Journal of the Association for*
736 *Research in Otolaryngology*, 19(2):181–191.
- 737 Verschuere, E., Gillis, M., Decruy, L., Vanthornhout, J., and Francart, T. (2022). Speech understanding
738 oppositely affects acoustic and linguistic neural tracking in a speech rate manipulation paradigm.
739 *Journal of Neuroscience*, 42(39):7442–7453.
- 740 Visch-Brink, E., Van de Sandt-Koenderman, M., and El Hachoui, H. (2010). *ScreeLing*. Houten: Bohn
741 Stafleu Van Loghum.
- 742 Wallace, S. E. and Kimelman, M. D. (2013). Generalization of word retrieval following semantic feature
743 treatment. *Neurorehabilitation*, 32(4):899–913.
- 744 Wöstmann, M., Lim, S., and Obleser, J. (2017). The human neural alpha response to speech is a proxy
745 of attentional control. *Cerebral cortex*, 27(6):3307–3317.
- 746 Xu, N., Zhao, B., Luo, L., Zhang, K., Shao, X., Luan, G., Wang, Q., Hu, W., and Wang, Q. (2022).
747 Two stages of speech envelope tracking in human auditory cortex modulated by speech intelligibility.
748 *Cerebral Cortex*, 33(5):2215–2228.
- 749 Zan, P., Presacco, A., Anderson, S., and Simon, J. Z. (2020). Exaggerated cortical representation of
750 speech in older listeners: mutual information analysis. *Journal of Neurophysiology*, 124(4):1152–1164.

751 Zou, J., Xu, C., Luo, C., Jin, P., Gao, J., Li, J., Gao, J., Ding, N., and Luo, B. (2021). θ -band cortical
752 tracking of the speech envelope shows the linear phase property. *eNeuro*, 8(4).